Molecular Crystals and Liquid Crystals Science and Technology. Section A. Molecular Crystals and Liquid Crystals
Publication details, including instructions for authors and subscription information:
http://www.tandfonline.com/loi/gmcl19

Electrical Switching and Memory Phenomena in Al/[TBA$_y$Ni(DMID)$_2$]/Cu System

Sheng-Gao Liu [a], Yun-Qi Liu [a] & Dao-Ben Zhu [a]
[a] Institute of Chemistry, Academia Sinica, Beijing, 100080, P.R. of China

Version of record first published: 04 Oct 2006.

To cite this article: Sheng-Gao Liu , Yun-Qi Liu & Dao-Ben Zhu (1996): Electrical Switching and Memory Phenomena in Al/[TBA$_y$Ni(DMID)$_2$]/Cu System, Molecular Crystals and Liquid Crystals Science and Technology. Section A. Molecular Crystals and Liquid Crystals, 281:1, 229-243

To link to this article: http://dx.doi.org/10.1080/10587259608042247

Mol. Cryst. Liq. Cryst., 1996, Vol. 281, pp. 229–243
Reprints available directly from the publisher
Photocopying permitted by license only

Electrical Switching and Memory Phenomena in Al/[TBA]$_y$[Ni(DMID)$_2$]/Cu System

SHENG-GAO LIU , YUN-QI LIU and DAO-BEN ZHU

Institute of Chemistry, Academia Sinica, Beijing 100080, P.R. of China

(Received May 10, 1995; Revised September 4, 1995; in final form July 17, 1995)

A sandwich structure of Al/[TBA]$_y$[Ni(DMID)$_2$]/Cu shows a bistable and reproducibe electric field-induced switching and memory phenomenon (TBA = tetrabutylammonium, DMID = 1,3-dithiole-2-one-4,5,-dithiolate). Preparation, characterization and electrical properties of this organic thin film materials are reported with those of the related materilas. The current-voltage (I-V) characteristics of Al/[TBA]$_y$[Ni(DMID)$_2$]/Cu reveal an abrupt decrease in resistance form a high to a low impedance state at a electric field strength of about 2400 V/cm for a 5 μm thick film sample. Switching with high-power dissipation yields a low-impedance memory state which can be erased by the application of large currents, typically 3–10 mA (0.3–1.0 A/cm^2), in either direction. In addition, the high-resistance state could also be re-established by allowing the device to remain for extended periods of time without an external electric field. The character of the switching from a high to a low impedance state in this organic charge transfer complex is same to the organic charge transfer complexes of M-TCNQ type (M = Cu, Ag; TCNQ = 7,7,8,8-tetracyano-*p*-quinodimethane). However, this contraster to the behavior observed in Al/[TBA]$_{0.9}$[Ni(DMID)$_2$/Pt system.

Keywords: Multi-sulfur bis (1,2-dithiolene) metal complex, DMID, thin film, organic semiconductor, electical switching, memory effect, molecular electronic device.

INTRODUCTION

The state-of-the-art technology of inorganic semiconductors is developing towords the direction of diminishing dimensions of device structures to utilize the quantum confinement effect. However, as the size of the microstructures is reduced to a subnanometer scale, technical problems in the device fabrication become increasingly serious[1]. Meanwhile, the concept of molecular devices (MD) or molecular electronic devices (MED) was sprouted out with a hope of utilizing "natural quantum confinement effect" in organic molecules and molecular aggregates. Organic compounds, such as organic macromolecules, organometallic compounds, polymers, or even biological molecules that can control or modify electrical and/or oprical signals are a viable alternative to the traditional inorganic because of their rather small size, abundance, diversity, ease of fabrication, and potential low cost. For example, the typical dimensions of organic molecular structures (10 to 100 Å) are 2 to 3 orders of magnitude smaller than existing and proposed devices developed by the current state-of-the-art lithographic techniques. Furthermore, organic semiconductors can offer an additional features in that it is possible to control the electronic and/or optical properties of an organic device by altering or tailoring the organic molecular structure before fabricating the device.

In the field of molecular electronic switches, the use of organic thin films has been early suggested by A. R. Elsharkawi *et al.*,[2] V. I. Stafeev *et al.*,[3] H. Carchano *et al.*,[4] J. Kevorkian *et al.*,[5] and A. Szymanski *et al.*[6] However, the electrical characteristics of these materials were erratic in nature or not readily reproducible, further, these devices disclose switching at impractical voltage or current levels and do not mention high speed, nanosecond switching. In 1979, R. S. Potember *et al.*[7] reported bistable, reproducible, and nanosecond electical switching between resistance states in polycrystalline organometallic charge-transfer complex films of Cu-TCNQ (TCNQ = 7,7,8,8,-tetracyano-*p*-quinodimethane). Since then, electrical, optical and opto-electronic switches have been demostrated by many different authors,[8-12] and furthermore the switching effect in Cu-TCNQ films has been frequently referred to as a prototype of a molecular electronic device. To our knowledge, at least three distinct classes of current switching effects have been reported so far and most of the previously reported work have been done on thin film structures[7,13-15] with the exception of the work done in G. Saito's group,[16] in which they reported the current switching effect associated with the intrinsic negative resistance effect[17-18] in various mixed–stacked organic charge transfer (CT) crystals.[16-19]

Recently we have reported a novel kind of reproducible, bistable, electric field-induced electrical switching and memory properties observed in a sandwich structure of Al/$[TBA]_{0.9}[Ni(DMID)_2]$/Pt in this journal (TBA = tetrabutylammonium, DMID = 1,3-dithiole-2-one-4,5-dithiolate).[15] In order to extend the research of this system and investigate the effect of the substrate on the physical properties, we studied other sandwich structures of thin film materials derived from the charge transfer complex of $[TBA]Ni(DMID)_2]$. The thin film materials were electrically deposited on either metallic copper or indium-tin oxide (ITO) substrates. In the sandwich structures of Al/$[TBA]_x[Ni(DMID)_2]$Cu and Al/$[TBA]_y[Ni(DMID)_2]$/Cu, bistable and reproducible electric field-induced switching and memory phenomena were observed, where the $[TBA]_x[Ni(DMID)_2]$ and $[TBA]_y[Ni(DMID)_2]$ films were electrically deposited on an anodic and a cathodic metallic copper substrates respectively with galvanostatic conditions. In this paper, we will report the preparation, characterization and electrical properties of these new thin film devices. The effects of the substrate on the switching and memory properties were observed and some comparison was made between the sandwich structures of Al$[TBA]_X[Ni(DMID)_2]$/Cu (sample (1)), Al/$[TBA]_Y[Ni(DMID)_2]$/Cu (sample (2)), Al/$[TBA]_z[Ni(DMID)_2$/ITO (sample (3)) and Al/$[TBA]_{0.9}[Ni(DMID)_2]$/Pt (sample (4)).

EXPERIMENTAL

Precursor charge transfer complex of $[TBA][Ni(DMID)_2]$ was synthesized as described by us.[20] The basic configuration of the device is as same as the reported one.[15] Film materials studied here were grown on either pure copper substrates or conductive glasses covered with ITO and all films were electically deposited on the substrates with galvanostatic conditions. For the film growth experiments, high-purity copper strips ($2 \times 1\ cm^2$) were firstly polished by using metallographic polishing paper from 0 down to 4/0, followed by cleaning with acetone to remove sanding particles and

organics from the surface, then cleaned by dipping in 1:1 HNO_3 aqueous solution, and finally washed with distilled water and acetone, dried under vacuum and used immediately to grow the films. The conductive glasses covered with ITO were commercially available and washed with acetone to remove any contaminants from the surface perior to use.

For Al/$[TBA]_x[Ni(DMID)_2]$/Cu(1) and Al/$[TBA]_y[Ni(DMID)_2]$/Cu(2) systems, fabrication of the devices consists of firstly immersing a cleaned copper metal foil, as treated above, in a solution of dry, degassed, and freshly distilled acetonitrile which has been oversaturated with the precursor metal bisdithiolene complex of $[TBA][Ni(DMID)_2]$.[20] In one case (1), the film was electrodeposited on an anodic Cu substrate under a constant current of 10 μA for about 3 h at room temperature. The cathode was graphite. In another case (2), the film was electrodeposited on a cathodic Cu substrate under a constant current of 5 μA for about 20 h at room temperature. The anode was platnium. For both cases, the two component structure was then gently washed with additional acetonitrile or acetone to remove any excess of the precursor molecules and dried under vacuum to remove any traces of the solvent. To prepare the samples for electrical characterization, top metal electodes of aluminium were evaporated onto the surface of the films under vacuum forming $1 \times 1\ mm^2$ contacts. No further treatment was performed after a three component structure was complete and the contact adherence was excellent.

For the Al/$[TBA]_z[Ni(DMID)_2]$/ITO (3) system, fabrication of the device consists of immersing an ITO substrate in a solution of dry, degassed, and freshly distilled acetonitrile which has been oversaturated with the precursor metal bisdithiolene complex. The film was deposited on an anodic ITO substrate (about 2 cm in diameter) under a constant current of 25 μA at room temperature.The cathode was graphite. After a desired ammount of time, a black film was formed on the surface of the ITO substrate. The film can be grown to a thickness of more than 10 μm in a matter of hours. Once the film has been grown to the desired thickness, the growth process was terminated by removing the substrate containing the organic layer from the acetonitrile solution. The bilayer structure was then gently washed with acentone to remove any excess precursor molecules and dried under vacuum to remove any traces of the solvent. A three component structure was complete when a top metal electrode of aluminium ($1 \times 1\ mm^2$) was evaporated on the organic thin film under vacuum.

All solvents used were purified and degassed according to standard methods perior to their use.

UV-Vis spectra was recorded on a HITACHI 340 spectrophotometer at room temperature.

X-ray diffraction (XRD) measurements were carried out at room temperature on a Dmax-3B diffractometer using a CuKα radiation. The X-ray source was operated at 40 kV and 30 mA. Scan speed was 2 deg/min.

Scanning electron microscopy (SEM) was done using a HITACHI S530 microcopy. The accelerator voltage was 25 keV with a working distance of about 10 mm.

Infrared spectra were recorded on a Nicolet Magna IR 750 Fourier Transform Infrared (FT-IR) spectrophotometer in the region of 4000–400 cm^{-1} as KBr pellets with scans of 32 at room temperature. Micro reflectance FT-IR spectra were recorded on a Nic-Plan FT-IR Microsope and Magna IR 750 (Nicolet) Fourier Transform

Infrared spectophotometer in the region of 4000–650 cm^{-1} with 500 scans at room temperature. The spectral accuracy and resolution was better than 1 cm^{-1}.

The DC current-voltage (I–V) characteristics were measured in the standard manner in air. The three component structure was connected through two external contact wires in series with a DC voltate source (voltage range 0–30 V) and a 510-Ω load resistor. The I–V curve was recorded on an X-Y recorder. In general, one contact wire was connected to the top electode by silver conducting paste or by liquid metals of mercury, gallium, or gallium-indium eutectic or directly by pressure contacting and another one connected to the conductive substrate by silver conducting paste or directly by pressure contacting so that the current flowed vertically through the film material.

RESULTS AND DISCUSSION

Materials

In order to extend the research and investigate the effect of the substrate on the electrical properties as well as other physical characteristtics, we prepared three more kinds of films on different substrates, metallic copper and conductive galss covered with ITO, with different electrochemical conditions in addition to the previously reported one,[15] as is tabulated in Table I.

Although we have performed elemental analysis on the bulk of the film (4) in the previously reported paper[15] in which the film growth condition was similar to those of the films (1)–(3), it was very hard for us to perform elemental analysis on the bulk of the films (1)–(3) on this occasion. So it is hard to evaluate the exact value of x, y, and z for the films (1), (2) and (3), respectively. However, it can be anticipated that the film (1) which was grown on an anodic copper substrate may have a different composition and physical characteristics from that of the film (2) which was grown on a cathodic copper substrate, which are discussed as follows.

Figure 1 is composed of Scanning Electron Micrographs (SEM) of the film (1)–(4). Comparing these graphs to one another, we can notice that the micrographs of the films (1) and (2) are quite different not only from that of the film (3), but also from that of the film (4).[15] However, the micrograph of the film (3) is similar to that of the film (4) in

TABLE I

The electodes used in the electrodeposition process and other film growth parameters

Flim	Composition	Anode	Cathode	Current (μA)	Time (h)	Temp. (°C)	Relative humidity of air
(1)	$[TBA]_x[Ni(DMID)_2]$	Cu	graphite	10	3	25	57
(2)	$[TBA]_y[Ni(DMID)_2]$	Pt	Cu	5	20	28	60
(3)	$[TBA]_z[Ni(DMID)_2]$	ITO	graphite	25	3	29	60
(4)[a]	$[TBA]_{0.9}[Ni(DMID)_2]$	Pt	graphite	25	3	28	60

[a] refer reference [15].

addition to that the film (4) is more tightly packed than the film (3). In addition, the micrograph of the film (1) is slightly different from that of the film (2). This may be explained as the partial electrolysis of the anodic copper metal during the film electrodeposition process. Typical film thicknesses for all the films (1)–(4) were 5–10 μm.

X-ray diffraction of the film materials showed them to be either very badly crystalline (films (1) and (2) or even amorphous (film (4)), as is shown in Figure 2. These are in good accordance with their SEM results.

Micro reflectance FT-IR spectral analysis.

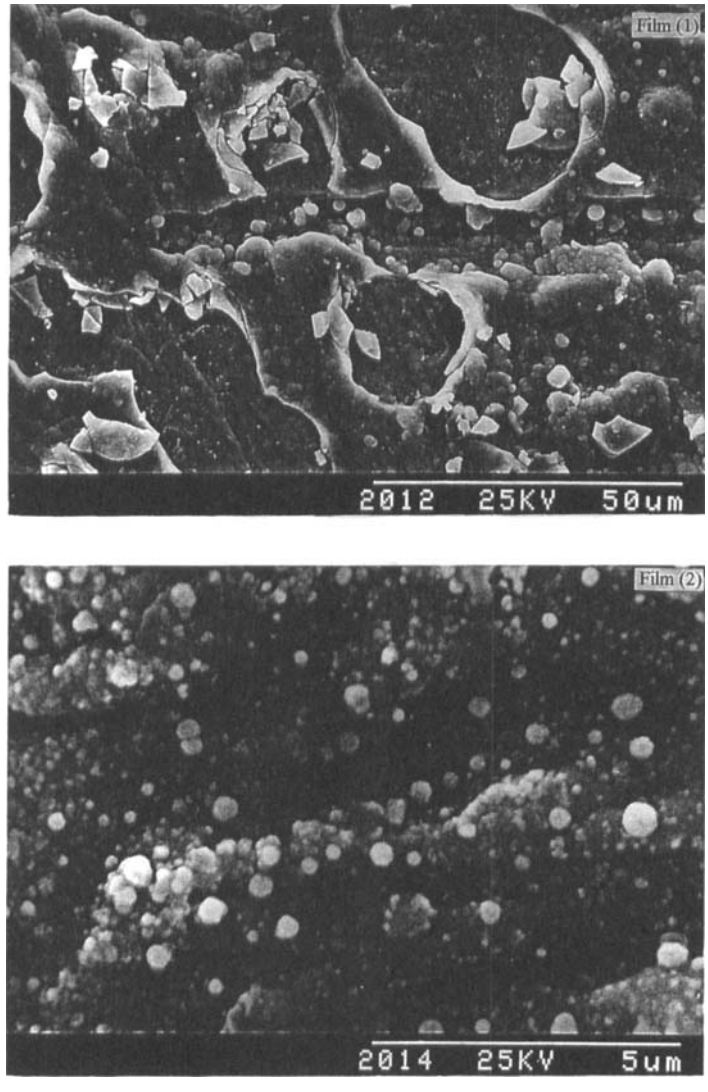

FIGURE 1 Scanning Electron Micrographs of the films (1)–(4).

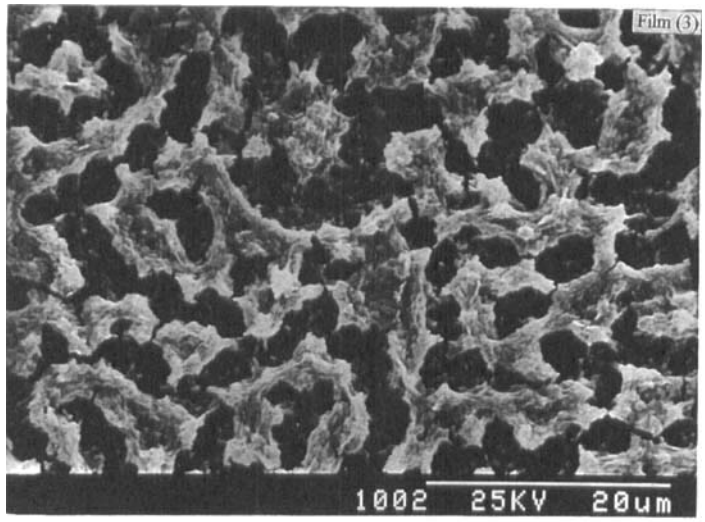

(c)

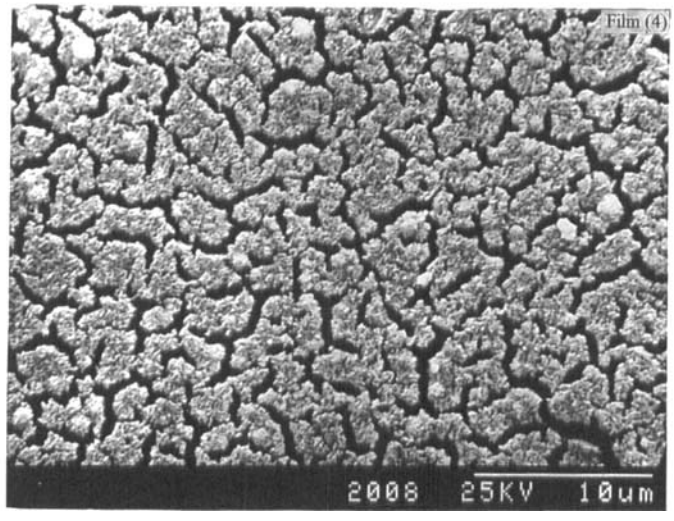

(d)

FIGURE 1 *(Continued).*

Figure 3 shows micro reflectance FT-IR spectra of the films (1), (2), and (4) in comparison with that of the precursor charge transfer complex. The spectra were measured on the surface of the films or on the pressed disk of the precursor compound. All of the spectra show the characteristic bands,[20] particularly the characteristic carbonyl group (C=O) stretching band, of the metal bisdithiolene complexes of DMID ligand. The characteristic bands of the C=O, C=C, C···S and C—S bonds in the bis (1,2-dithiolene) metal complex thin film materials lie within 1680-1590, 1470-1410, 1040-970, and 900-870 cm^{-1} range, respectively. In the region of 1250-1100 cm^{-1} appears vibrational absorption (s) of the C—C single bonds of the alkyl group in the tetrabutylammonium ion.

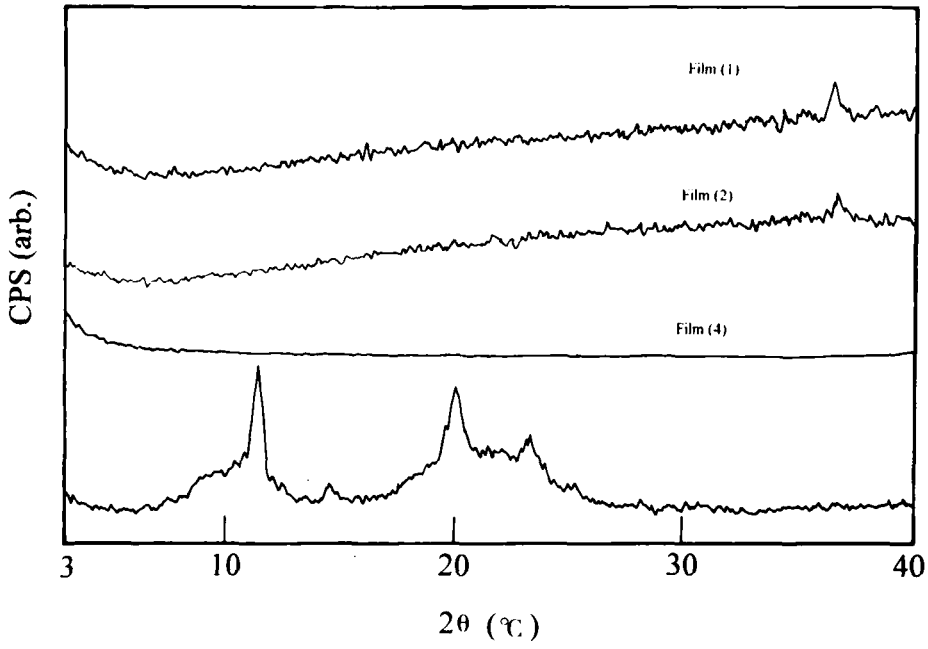

FIGURE 2 X-ray diffraction patterns of the films (1), (2), (4) and the polycrystalline precursor complex of [TBA][Ni(DMID)$_2$] (bottom) with X-ray diffraction peaks tabulated as follows

Material	2θ(°C)	d	Intensity
Film (1)	36.54	2.457	252
Film (2)	36.64	2.450	221
Film (4)[a]	–	–	–
Precursor compound	11.44	7.728	333
	20.06	4.422	295
	23.34	3.808	201

[a] Amorphous, this pattern is same to that of the film (3).

It should be noted that both the shape and the position of the C=O stretching peak in the reflectance band for the films (1) and (2) are not only different from that of the film (4), but laso different from that of the precursor complex, either reflectance or transmission measurements. Some peaks in the reflectance band for the films (1), (2) and (4) and the precursor compound are listed in Table II.

It shows that the C=O stretching mode for the film (2) shifted to a lower frequency by about 30 cm^{-1} in comparison with that for the film (4) and for the precursor compound as well and to a lower frequency by about 10 cm^{-1} in comparison with the film (1). This may be explained as partial reduction of the presursor complex on the cathodic copper electrode. The C=O stretching frequency for the film (4) shifted to a higher frequency by about 20 cm^{-1} in comparison with that of the film (1). Hence, the C=O stretching frequency in these thin film materials seems to be in the series of (4) > (1) > (2).

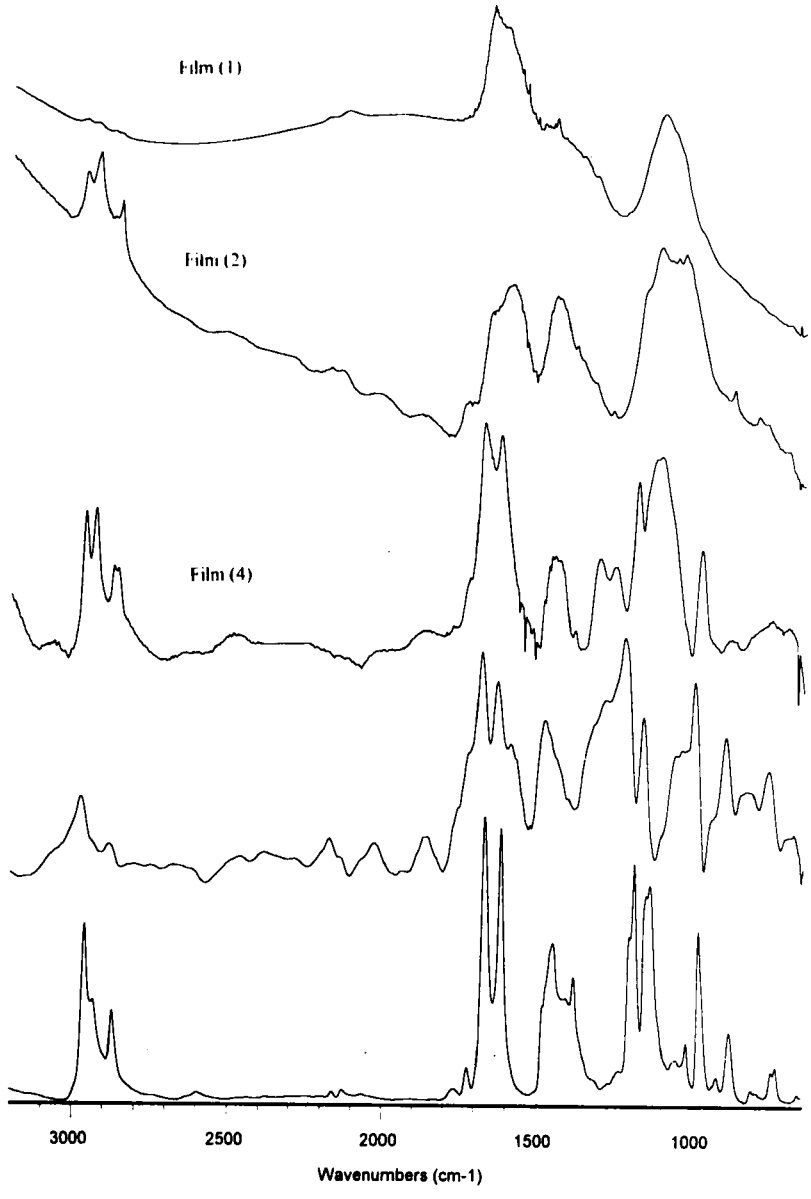

FIGURE 3 Micro reflectance FT-IR spectra of the films (1), (2), and (4) as well as the precursor complex of [TBA][Ni(DMID$_2$] (pressed disk) (second from bottom), and the FT-IR transmission measurement on the precursor complex (KBr pellet) (bottom). The spectra were undertaken baseline correction in addition to those of the films (1) and (2). The unit of the ordinate axis is absordance (arb).

UV-Vis Spectral Analysis

The UV-Vis spectra of the precursor compound [TBA][Ni(DMID)$_2$] and the film (3) are shown in Figure 4. One of our interests for the study of UV-Vis spectrum comes

TABLE II

Some characteristic peaks in reflectance bands in the films (1), (2), and (4) and in the precursor complex of [TBA][Ni(DMID)$_2$]

Material	C—H	C=O	C=C	C⋯S	C—S
Film (1)	2967 2933	1649 1612	1449 1415		873
Film (2)	2957 2924 2859	1640 1592	1439	1033	876
Film (4)[a]	2957 2927 2863	1670 1620	1443	977	880
Precursor compound	2968 2876	1678 1622	1462	991	898

[a] from reference [15].

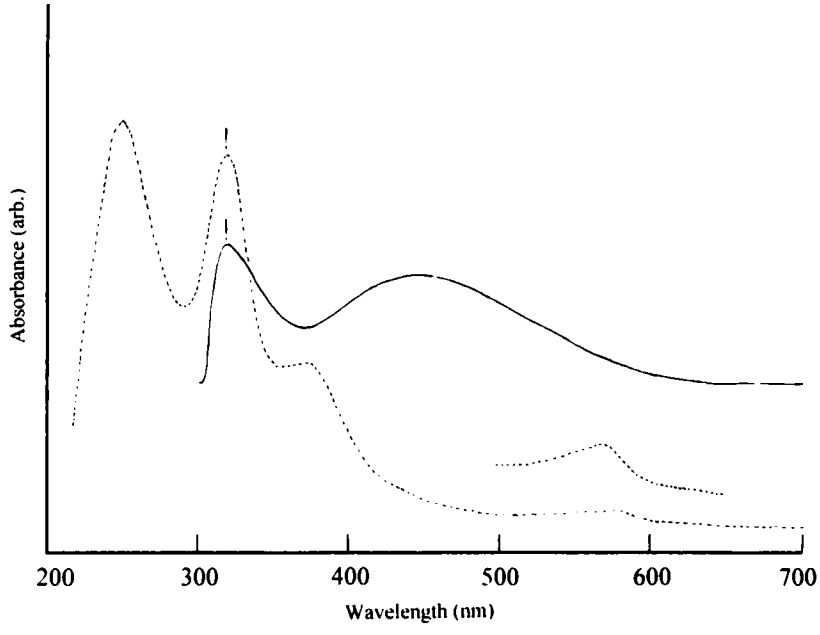

FIGURE 4 UV-Vis spectra of the precursor complex in methanol solution in a 1 cm quartz cuvette with the solvent as reference (dashed line) and the film (3) with the substrate as reference (solid line).

from the π-elctronic delocalization over the ligand which may be vital for the solid state properties of the materials. In the case of the film material (3), the spectra show one of the characteristic bands[20] of the carbonyl group at about 320 nm and another broad absorption band centered at about 448 nm, which may be assigned to the π-electronic delocalization band. This delocalization band could be an important evidence for the *d* orbitals of the central metal ion to interact with the π orbitals on the two ethylene double bonds through the lone-pair electrons on the inner four sulfide bridges, and the

π orbitals on the ethylene double bonds then interact with the π orbitals on the two periphery carbonyl groups through the lone-pair electrons on the outer four sulfide bridges.[20] Considering this kind of interaction between d and π orbitals, we look into the difference between the spectra of the film material (3) and the precursor compound, we can notice that this characteristic band due to the π-electonic delocalization over the ligand through the central metal ion and the eight sulfide bridges blue-shifts from about 448 nm for the former to about 370 nm for the latter. This may be tentatively explained as the difference of the d-π interactions in these two systems due to the different stoichiometries between the systems and the difference of the intermolecular interactions between the film material (3) in solid state and the precursor compound in solution. Further work will be done to clarify this point. The weak band at around 580 nm for the precursor complex may be assigned to the d-d transition from the central chelating metal ion.

Electrical switching and memory properties

After top metal electrodes of aluminium (1×1 mm^2) were evaporated onto the organic thin films (1)–(4) under vacuum, three component structures were complete. Table 3 presents the four different samples studied.

DC current-voltage (I–V) characteristics were measured in the standard manner in air, as shown in Figure 5. Using a copper probe station, the sample was connected in series with a DC voltage source (0–30 V) and a load resistor (typically 510 Ω). In general, one copper probe was placed on the fabrication electrode and another on the evaporated metal electrode (metal pad) so that the current flowed vertically through the sample. Sample voltage drop and current were recorded on an X-Y recorder.

For sample (3), we could not observe any switching phenomena. Before suffering puncture, the device was in a high-impedance "OFF-state" all the way with the increase of the applied voltage from 0 to 30 V in either polarity for a 10 μm thick film sample.

In contrast, for sample (2), memory switching behavior was observed. Figure 6 shows a typical DC I–V curve of one such unit having a $[TBA]_Y[Ni(DMID)_2]$ layer which was grown on the cathodic copper substrate and was approximately 5 μm thick. The electrical characteristics were essentially independent on the direction of the current flow. Typical behavior was as follows. At the outset, the device was in an ohmic high-resistance "OFF-state" provided the field strength across the sample did not exceed a certain threshold value (around 2400 V/cm in this case, corresponding to V_{th}

TABLE III

Samples and their fabrication electrodes and electrical switching behavior

Sample	Evaporated Electrode	Fabrication Electrode	Film thickness (μm)	Switching Behavior As grown (ρ^a_{rt} Ωcm)	Switch to (ρ^a_{rt} Ωcm)
(1)	Al/$[TBA]_x[Ni(DMID)_2]$/Cu (anode)		10	OFF(7.7×10^3)→ON(1.2×10^3)	
(2)	Al/$[TBA]_y[Ni(DMID)_2]$/Cu (cathode)		5	OFF(1.2×10^5)⇌ON(8.0×10^3)	
(3)	Al/$[TBA]_z[Ni(DMID)_2]$/ITO (anode)		10	OFF(3.0×10^5) No switching	
(4)	Al/$[TBA]_{0.9}[Ni(DMID)_2]$/Pt (anode)		10	ON(3.0×10^3)⇌OFF(1.5×10^6)[15]	

[a] The resistivity (ρ) was calculated from the following equation in these cases:
$\rho = (V/Id) \times 10^5$ (I in mA, V in Volt, the film thichness d in μm).

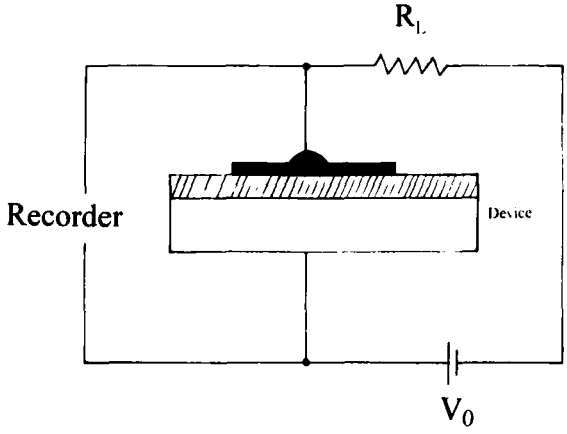

FIGURE 5 Schematic diagram of the current-voltage (I–V) curve measurementation on the devices (samples (1)–(4) (R_L: load resistor, V_0: DC voltage source, the configuration of the device is as same as the reported one in reference [15]).

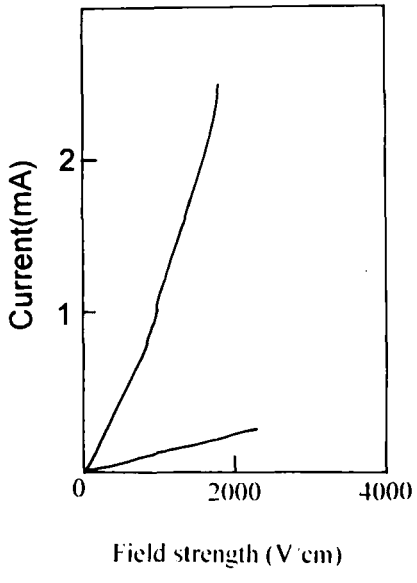

FIGURE 6 Typical DC I–V characteristic curve showing high- and low-impedance states for the sample (2).

of about 1.2 V). In this state, for small applied voltages of either polarity, the current was rather low (at maxima 0.2 mA), indicating a device resistivity of about $1.2 \times 10^5\ \Omega$.cm. When the applied field strength exceeded the threshold value, the device resistivity abruptly decreased to about $8 \times 10^3\ \Omega \cdot$cm, thus putting the device into a low-impedance "ON-state". The ratio of ρ_{off}/ρ_{on} was generally 10–100. The low-resistance "ON-state" is non-ohmic with a rise in the current to approximately 1.0 mA and a concurrent

decrease in the voltage to approximately 0.4 V. Once the device switched to the low impedance "ON-state", it remains in that state as long as external field is applied. When the applied voltage is removed, the device acted as a memory switch and remained in the low-resistance "ON-state". This memory state cab be erased and driven back to the high-impedance "OFF-state" by the application of large currents in either direction (typically 3–10 mA, i.e., 0.3–1.0 A/cm^2). In addition, the high-resistance state could also be reestablished by allowing the cell to remain for extended periods of time without an external electirc field. This is a few seconds up to dozens of minutes or even several hours, which depends on the duration of the applied field and the amount of power dissipated in the sample while in the "ON-state".

Several important points should be noted. First of all, the device switched from a high to a low resistance state only when the applied field strength exceeded a certain critical value. The polarity of the applied potential is unimportant. Furthermore, the device could be switched OFF only when an above-threshold current (of either direction) was attained. This is consistent with the behavior of the memory switching elements reported by P. O. Sliva *et al.*,[21] where the polarity is also unimportant and the "OFF-state" can be recovered by applying large currents in either direction, physical shock, or rf discharge. However, this is constrasted to the behavior of the memrory switching elements reported by E. T. Zellers *et al.*,[14] where the device switching from a high to a low resistance state only when a positive potential was applied to the evaporated metal gate and the "OFF-state" can be recovered only by reversing the polarity of the applied electirc field. Second, the switching effect is insensitive to air, moisture, and light and the device is stable over a long period of time (at least a few months). This is consistent with the memory switching effect observed in the sample (4).[15].

Preliminary tests have revealed the following. Some results concerning the device durability are available. Several points on the sample (2) or different samples with the same film growth parameters as that of the sample (2) were sujected to repeated switching tests. The samples could be switched more than 20 switching cycles before suffering catastrophic failure using the same points in a sample.

In addition, for the sample (1), typical behavior was as follows. At the outset, the cell was in non-ohmic high-resistance "OFF-state" provided that the field strength across the sample did not exceed a certain threshold value (around 2700 V/cm in this case, corresponding to V_{th} of about 2.7 V for a 10 μm thick film sample). In this state, for small applied voltages of either polarity on the evaporated metal gate, the current was somewhat low, indicating a device resistivity of about 7.7×10^3 Ωcm. When the applied voltage exceeded the threshold value, the device resistivity abruptly dropped to approximately 1.2×10^3 Ωcm, thus putting the device into a low-resistance "ON-state". The ratio of ρ_{off}/ρ_{on} was generally 2–10. This low-resistance "ON-state" is non-ohmic with a rise in the current to approximately 5.6 mA and a concurrent decrease in the voltage to approximately 0.65 V. Once the device switched to the low impedance "ON-state", it will remain in that state indefinitely whether the external field is applied or removed. Furthermore, this low impedance "ON-state" could not be erased by the application of large currents in either direction (up to 20 mA).

It should be pointed out that some differences could be observed between the samples (1) and (2) as described above. On the other hand, there are also some

similarities between these two systems. The most important similarity is that they both initially switch from a low conductance to a low impedance state, i.e., from the "OFF" to the "ON" state, at an above-threshold electric field strength. This is similar to the switching effects observed in the metal charge-transfer salts of M-TCNQ,[7] M-TNAP (TNAP = 11,11,12,12-tetracyanonaptho-2,6-quinodimethane)[13] and so on, in which the switching effects can be observed from the "OFF" state to "ON" state. However, it is contrasted to that observed in the sample (4)[15], in which a rapid switching is observed from the "ON" to the "OFF" state when an applied field across the sample surpasses a threshold value of about 2400 V/cm for a 10 μm thick film sample. In addition, it has been observed that once the device is in the "OFF" state, it will remain in that state as long as an external field is applied. In every case studied, the device could eventually return to its initial low-impedance "ON" state after the applied field was removed. This memory state can remain intact from a few minutes to several hours after the applied potential was removed and it can also be immediately removed by application of a high voltage in either direction. The voltage required to switch back to the initial state appeared to be directly proportional to the film thickness, duration of the applied field, and the amount of power dissipated in the sample while in the "OFF" state.

The difference in the switching behavior between these systems may be mainly due to the difference of their switching mechanism. In the sample (4), the postulated mechanism is believed to be a field-induced, solid-state, reversible electrochemical redox reaction which results in switching in the reported structure wherein integer oxidation state species or simple salts are in equilibrium with the initially highly conductive salt as exemplified by the following equation:[15]

$$n\{[\mathrm{TBA}]_x[\mathrm{Ni(DMID)_2}]\} \underset{\text{Electric field}}{\rightleftharpoons} m\cdot x\{[\mathrm{TBA}][\mathrm{Ni(DMID)_2}]\} + (1-x)\cdot m\{[\mathrm{Ni(DMID)_2}]\} + (n-m)\{[\mathrm{TBA}]_x[\mathrm{Ni(DMID)_2}]\}$$

low impedance "ON" state — high impedance "OFF" state

However, in the sample (2), we do not know the exact switching mechanism at the present stage. But, we could at least suggest that it could be bulk rather than interfacial oriented. The main justification for this is that the bistable behavior was observed when an above-threshold voltage of either polarity was achieved and the behavior could be observed on other systems, such as in the sample (1).

It should be noted that, despite the difference in their switching behavior, the threshold electric field strength for both Al/$[\mathrm{TBA}]_y[\mathrm{Ni(DMID)_2}]$/Cu(2) and Al/$[\mathrm{TBA}]_{0.9}[\mathrm{Ni(DMID)_2}]$/Pt(4) systems seems to be independent on the substrate as well as the film thickness. This is consistent with the electrical switching behavior of the charge-transfer complexes of M-TCNQ type, where the magnitude of the applied field strength required to effect switching depends on the strength of the π-electron acceptor,

TABLE IV

Relationship between reduction potentials of the acceptor and field strength at switching threshold

Charge-transfer complex	Reduction potentials of the acceptor (V, E_1, *vs* SCE)	Approximate field of switching threshold (V/cm)
$[TBA]_y[Ni(DMID)_2]$	−0.28	2400
$[TBA]_{0.9}[Ni(DMID)_2]$[15]	−0.28	2400
CuTCNQ[22]	+0.17	5700
CuTNAP[22]	+0.20	8200
$CuTCNQF_4$[22]	+0.53	13000

as is evidenced by the value of the switching field strength of M-TCNQ, M-TNAP and so on, tabulated in Table IV.

SUMMARY

Novel charge transfer complex thin film structures have been described which demonstrate bistable memory switching behavior. The structure of $Al/[TBA]_y[Ni(DMID)_2]/Cu$ exhibits a rapid transition from a high impedance to a high conductance state and has a memory persistence of about a few seconds to dozens of minutes or even several hours and has a lifetime of more than 20 switching cycles. Some effects of the substrate on the electrical switching property as well as other physical characteristics were observed. On the one hand, in $Al/[TBA]_z[Ni(DMID)_2]/ITO$ system, no switching was observed eventhough the applied electric field reached to about 3×10^4 V/cm. On the other hand, in both $Al/[TBA]_x[Ni(DMID)_2]/Cu$ and $Al/[TBA]_y[Ni(DMID)_2]/Cu$ systems, a rapid switching was observed from the "OFF" to the "ON" state when an applied field strength across the sample surpasses a threshold value. This is contrasted to the behavior in the $Al/[TBA]_{0.9}[Ni(DMID)_2]/Pt$ system, in which the switching was observed from the "ON" to the "OFF" state when an applied strength across the sample surpasses a threshold value.

Acknowledgments

The authors wish to give special thanks to professor G. Saito (Kyoto University, Japan) for his valuable suggestions and gratefully acknowledge support by the National 863 Program from the China Commission for Science and Technology, the Key Funds of the Chinese Academy of Sciences and NNSF.

References

1. E. Corcorn, *Scientific American, November*, p. 47 (1990).
2. A. R. Elsharkawi and K. C. Kao, *Phys. Chem. Soc.*, **18**, 95 (1977).
3. V. I. Stafeev, V. V. Kuznetsova, V. P. Molchanov, S. S. Serov, V. V. Pospelov, E. I. Karakushan, S. V. Airapetyants and L. S. Gasanov, *Soviet Physics Semiconductors*, **2**, 642 (1965).
4. H. Carchano, R. Lacoste and Y. Segui, *Appl. Phys. Lett.*, **19**, 414 (1971).
5. J. Kevorkian, M. M. Labes, D. C. Larson and D. C. Wu, *Discussions of the Faraday Society*, (51), (1971).

6. A. Szymanski, D. C. Larson and M. M. Labes, *Appl. Phys. Lett.*, **14**, 88 (1969).
7. R. S. Potember, T. O. Poehler and D. O. Cowan, *Appl. Phys. Lett.*, **34**, 405 (1979).
8. R. S. Potember, T. O. Pochler and R. C. Benson, *Appl. Phys. Lett.*, **41**, 548 (1982)
9. R. C. Benson, R. C. Hoffman, R. S. Potember, E. Bourkoff and T. O. Pochler, *Appl. Phys. Lett.*, **42**, 855 (1983).
10. E. I. Kamitsos and W. M. Risen, *Solid State Commun.*, **45**, 165 (1983).
11. H. Hoshino, S. Matsushita and H. Samura, *Jpn. Appl. Phys.*, **25**, L341 (1986)
12. R. C. Hoffman and R. S. Potember, *Appl. Opt.*, **28**, 1417 (1989).
13. R. S. Potember, T. O. Pochler, A. Rappa, D. O. Cowan and A. N. Bloch, *J. Am. Chem. Soc.*, **102**, 3659 (1980).
14. E. T. Zellers, R. J. Roedel and F. Wudl, *J. Non-Crystalline Solids*, **46**, 361 (1981).
15. S. G. Liu, P. J. Wu, Y. Q. Liu and D. B. Zhu, *Mol. Cryst. Liq. Cryst.*, in press (1995).
16. Y. Iwasa, T. Koda, Y. Tokura, S. Koshihara, N. Iwasawa and G. Saito, *Appl. Phys. Lett.*, **55**, 2111 (1989).
17. Y. Tokura, H. Okamoto, T. Koda, T. Mitani and G. Saito, *Phys. Rev. B*, **38**, 2215 (1988).
18. Y. Iwasa, T. Koda, S. Koshihara, Y. Tokura, N. Iwasawa and G. Saito, *Phys. Rev. B*, **39**, 10441 (1989).
19. Y. Tokura, S. Koshihara, Y. Iwasa, H. Okamoto , T. Komatsu, T. Koda, N. Iwasawa and G. Saito, *Phys. Rev. Lett.*, **63**, 2405 (1989).
20. S. G. Liu, P. J. Wu, Y. F. Li and D. B. Zhu, *Phosphorus, Sulfur, and Silicon*, **90**, 219 (1994).
21. P. O. Sliva, G. Dir and C. Griffiths, *J. Non-Crystalline Solids*, **2**, 316 (1970).
22. R. S. Potember, T. O. Poehler and D. O. Cowan, *U. S. Patent*, No. 4, 507, 672, Mar. 26, 1985.